Investigation on the Effect of Temperature Excursion on the Helium Defects of Tungsten Surface by using Compact Plasma Device

S. Takamura†, T. Miyamoto†, Y. Tomita†, T. Minagawa† and N. Ohno††

Abstract The effects of temperature excursion on the helium defects of tungsten surface have been investigated by using compact plasma device AIT-PID. An initial stage of bubble formations has been identified with an order of smaller (sub-micron) bubbles and holes than those in the past in which the micron size is the standard magnitude. The radiation cooling has been detected when a blacking of tungsten surface coming from nanostructure formation is proceeding due to an increase in the emissivity up to almost 1.0 in the final stage. The temperature increase to the domain (～1600K) in bubble/hole formation from that in nanostructure formation has been found to bring a constriction in diameter and a reduction in length of fiber-form nanostructure.

1. Introduction

Helium defects of tungsten surface have been considered to be serious for all-metal plasma-facing components including first wall and divertor target plate in burning fusion plasma devices [1]. Helium bubbles and holes at high surface temperature more than about 1600K [2] and arborescent nanostructure at the temperature lower than about 1500K [3,4] are the typical morphology of damaged tungsten surface.

However, a large temporal change in temperature of tungsten surface may be anticipated in tokamak fusion reactor due to dynamic operation of tokamak discharge and various kind of relaxation phenomena including transient periodic enormous heat local like ELM. Therefore, the investigation on the effect of temperature excursion on the helium defects of tungsten becomes very important in terms of arcing, erosion and tungsten release from the surface under burning condition.

2. Experimental set-up

The device for the present study is called AIT-PID (Aichi Institute of Technology - Plasma Irradiation Device) has a machine structure shown in Fig 1, which is equipped with three

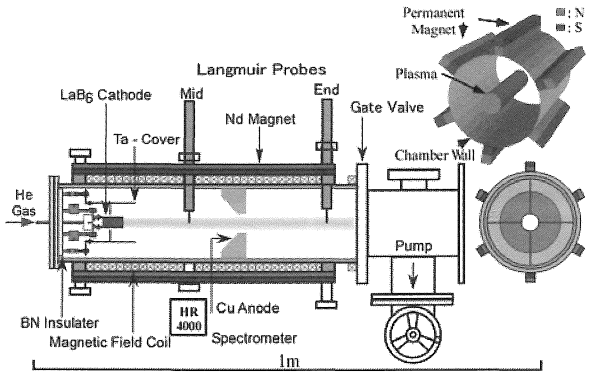

Fig.1 Experimental device – AIT-PID -.

pairs of neodymium permanent magnet bars (the cross section : 15 mm x 15 mm) composing a multi-cusp (poloidal mode number: 6) magnetic configuration and a solenoidal winding underneath the magnets producing a weak axial magnetic field up to 10 mT [5]. The intensity distributions of magnetic field perpendicular to the axis obtained by both the experiment using gauss meter and a numerical analysis are quite good in the agreement between these two. We have magnetic-free zone on the axis through which the produced plasma may path in the axial direction. The weak axial field may help the longitudinal transport of the plasma. At the end of this zone, the LaB_6 cylindrical cathode with the diameter of 20 mm is located, while the target for PWI is set at the mid position. An emission

†　愛知工業大学　工学部　電気工学科（豊田市）
††　名古屋大学　工学研究科（名古屋市）

spectrum has been obtained through the viewing port at the mid, showing a pure He plasma without any serious contamination.

At the moment we have succeeded in the discharge current of 25 A while the plasma density exceeds 1 x 10^{18} m^{-3} with a bulk electron temperature of 5 eV with a hot electron component of 10 % and the temperature of 40 eV. The ion flux to the target is around 1 x 10^{22} $(m^2s)^{-1}$.

3. Experimental results and discussions

The high density helium plasma has been obtained with a good radial confinement by using the multi-cusp magnetic field associated with a weak axial field. The helium ion irradiations on the powder metallurgy tungsten have been performed in this compact plasma device AIT-PID. The tungsten target plate(10 x 10 mm^2) was inserted into the central position of AIT-PID at the same axial locations as the scanning probe, but at the poloidally different port.

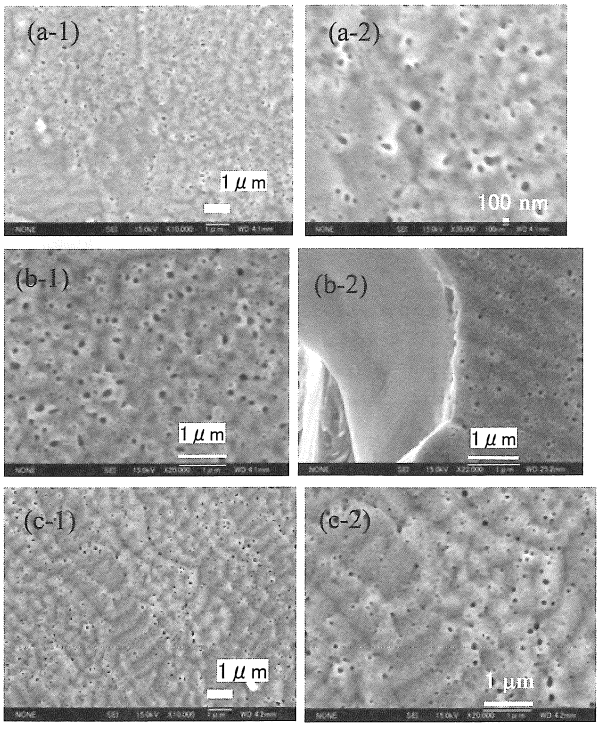

Fig.2 Bubbles/holes formation. The ion flux : 6.5～8.6 x$10^{21}$$(m^2s)^{-1}$. The ion bombarding energy is 25～30 eV. (a) T～1650K, Fluence F < 2.1 x $10^{25}$$m^{-2}$, (b) T～1700K, F = 4.6 x 10^{25} m^{-2}, (c) T～1600K, F = 7.7 x 10^{25} m^{-2}.

3.1 Initial stage of bubble/hole formation

The floating voltage (sheath voltage) of the target was found to be around 45 V which is fairly high owing to the presence of hot electron component. This determines the ion incident energy of 45 eV under the floating condition of the target plate. We can increase the surface temperature up to around 1700 K by biasing the target towards the plasma potential. The surface temperature is obtained by an infrared radiation thermometer (CHINO: IR-CAS) with the emissivity ε= 0.43. The wavelength of infrared ray is 0.9 μm with a Si detector. In this case the ion incident energy to the tungsten surface is decreased to 25～30eV by the biasing potential of around -20 V. The obtained surface morphology is shown in Fig. 2.

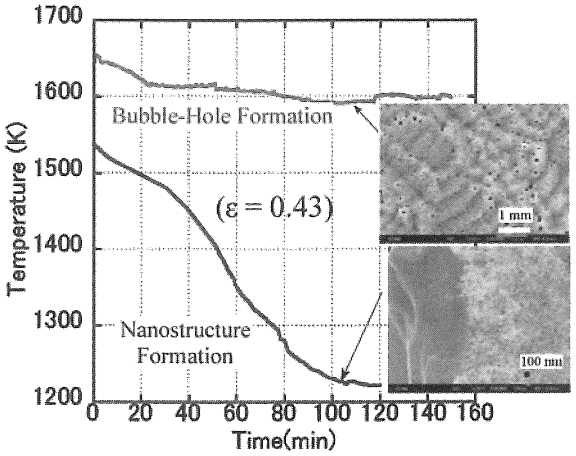

Fig.3 Typical temporal change in tungsten surface temperature for both bubble/hole formations range at higher temperature and nanostructure one at lower temperature

The bubble and holes are created, however the size of them is not as large as 1 micron as observed before, but an order of magnitude smaller than those [2, 6~8]. It means and initial stage of the development of bubbles and holes.

3.2 Temporal change in surface temperature

The typical temporal behaviors of tungsten surface temperature are shown in Fig.3 for both bubble/hole formation case and nanostructure one. The common feature is the temperature decrease in time. But we have a dramatic decrement roughly 300 K when the nanostructure is formed on the surface, while a modest decrease is detected when the bubbles/holes are produced there. It should be noted that the surface morphology is bifurcated at the surface temperature around 1600 K although there is a small change in ion incident energy by around 10 eV. In these observations the emissivity for infrared radiation thermometer is fixed at ε= 0.43. The blacking in color for nanostructured tungsten suggests a large increase in emissivity probably approaching to the value 1.0 [9, 10]. It means that the tungsten surface becomes an ideal black-body, which is also estimated from the observation of

well-developed tungsten surface morphology with enough

helium ion irradiation to have a saturations of surface temperature reduction, as shown in Fig.4.

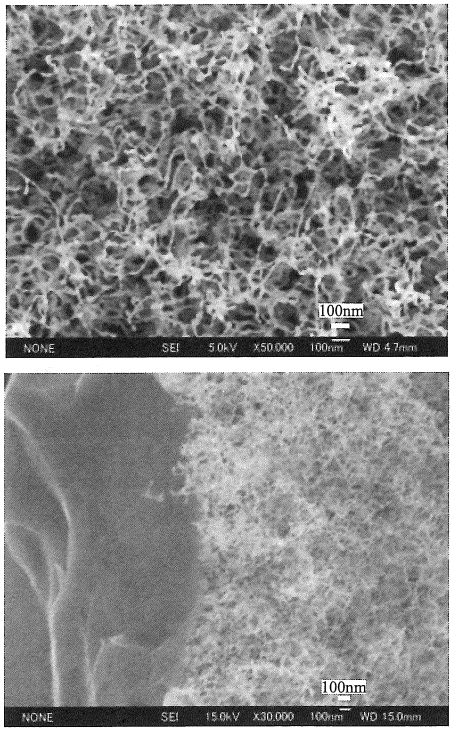

Fig.4 Surface morphologies of some typical well-developed nanostructure on the tungsten surface. The top picture shows the surface, while the bottom one does an oblique observation of broken edge.

On the other hand, the plasma heat load to the tungsten target would be maintained at the same level since the sheath thickness around 100 μm is much greater than the scale of nanostructure < 100nm. The temperature reduction is scaled as $(0.43/1.0)^{1/4}$ ~0.81 owing to the radiation power dependence $P_r = \varepsilon\sigma T^4$ so that 1530K x 0.81 = 1240K would be anticipated. Figure 3 shows a little bit lower temperature. But we note that this curve was obtained by fixing the emissivity of 0.43 so that a much more lower temperature would be expected. According to the high-frequency approximation of Planck's law, we obtain the following equation:

$$I'(\lambda,T) = \frac{2hc^2\varepsilon}{\lambda^5} e^{-\frac{hc}{\lambda\kappa T}} = Ae^{-\frac{16.0\times10^3}{T[K]}}, \quad (1)$$

where λ = 0.9 μm. The temperature difference measured with ε = 1.0 and 0.43 is given by

$$\Delta T = T_{1.0} - T_{0.43} = -0.84\frac{\overline{T}^2}{16.0\times10^3}, \quad (2)$$

where $\overline{T} = \sqrt{T_{1.0} \times T_{0.43}}$. When $\overline{T} = 1200K$, then we obtain $\Delta T = -76K$.

In order to confirm the reductions in temperature, the another type of infrared radiation thermometer (CHINO: IR-CAQ2CS) with three combinations of wavelength and detector: 1.55(InGaAs), 1.35(InGaAs) and 0.9μm(Si), when we assume ε(1.55μm) / ε(0.9μm) = 0.7 and ε(1.55μm) / ε(1.35μm) = 1.0. The starting temperature of 1410K is decreased down to 1100K with temperature reduction of 310K. So it is concluded that the nanostructure formation increases the radiation loss to bring some cooling of tungsten target under the same background plasma conditions.

We note that the floating potential of the tungsten target tends to become negatively deep from -35 down to -43 in time correlated to the decrement of surface temperature. The plasma potential of about +5 V with respect to the vacuum chamber would not change much. The sheath voltage of about 40 V at floating condition is fairly high considering the electron temperature of around 4 eV since $V_f \sim 4T_e$ ~16 V in helium plasma. But the hot electron component of 40 eV with the fraction of 10 % would explain such a high floating voltage. Anyway, an observable change in floating potential suggests some effect of nanostructure on sheath formation on the tungsten surface in spite of the above arguments concerning the scale comparison.

3.3 Effects of increased heat load on nanostuructured surface

After obtaining well-developed nanostructured tungsten specimens with two-hours exposure to helium plasma, the surface temperature of these tungsten target plate is increased to around 1600 K by adjusting the plasma parameters and biasing the targets towards the plasma potential but still with the ion incident energy larger than 15 eV and keeping the ion flux density of around 1 x 10^{22} $(m^2s)^{-1}$. The surface morphology of these specimens with additional heat load is found to be changed seriously and very rapidly in time, depending on the arrived surface temperature T_{surf} and the time period for additional irradiation.

The most important morphological changes are an enhancement in thickness and a reduction in length of nanostructured tungsten fiber with helium bubble inside [11] as

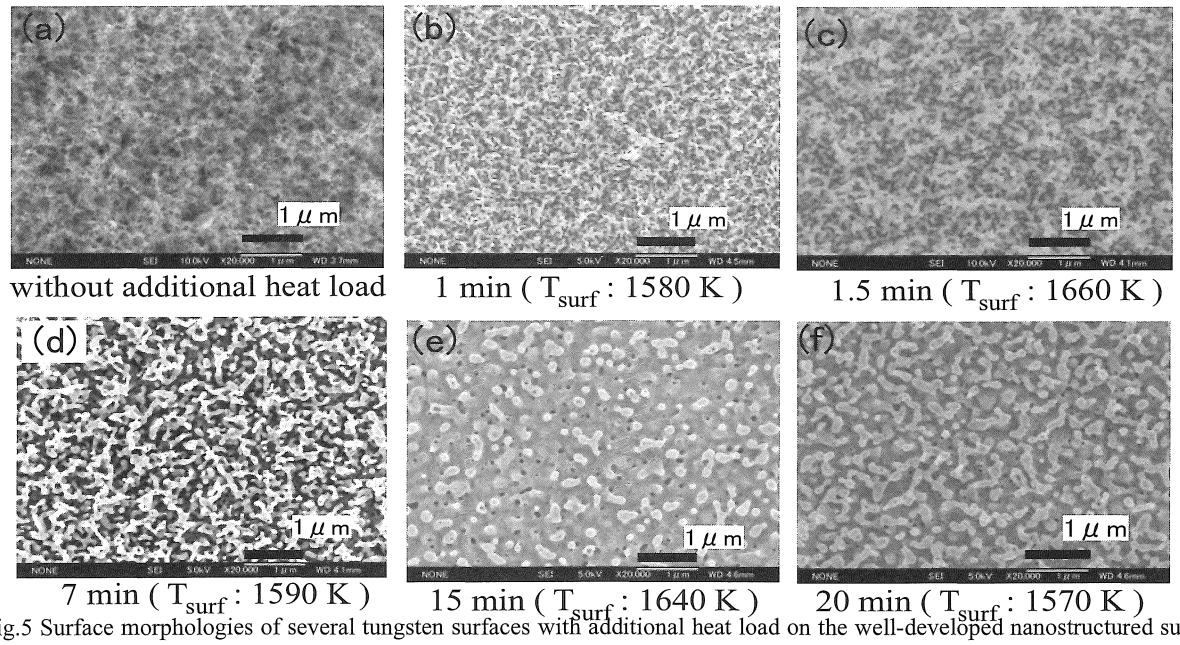

Fig.5 Surface morphologies of several tungsten surfaces with additional heat load on the well-developed nanostructured surfaces. T_{surf} is the surface temperature during additional heat load and the time in minute is the time period for that

shown in Fig. 5. Such changes become large as the time period increases and the T_{surf} becomes high. This kind of behavior may be partly explained by helium leakage from the bubbles and the swelled fibers are shrunk.

During the temperature excursion, the visible light emission of tungsten atomic line WI 498.3nm has been carefully checked with spectrometer whether it could increase or not. An increase could show a possible tungsten release to surrounding helium plasma from the damaged surface. However, no increase has been detected In these experimental conditions we do not have any tungsten release even with some shrinkage of tungsten nano-fibers.

4. Summary and conclusions

The following new findings have been obtained in this study for the helium defect on tungsten surface by using the compact plasma device AIT-PID:

1) An initial stage of macroscopic bubble / hole formations with an order of smaller (sub-micron) bubbles and holes than that in the past.
2) The radiation cooling due to a blacking of tungsten surface coming from nanostructure formation in which the emissivity approaches up to almost 1.0 in well-developed nanostructured surface.
3) A constriction in diameter and a reduction in length of fiber-form nanostructure tungsten textile by increasing the temperature to the domain of bubble / hole formation (~ 1600 K) from that of nanostructured one.

Acknowledgements

This research was supported by the Ministry of Education, Science, Sports and Culture, Grant-in-Aid for Scientific Research (B), 20360414 from JSPS. The authors would like to thank H. Iwata of Electrical Engineering in A.I.T. for his help on FE-SEM manipulation.

References

[1] A. Loarte et al., Nucl. Fusion **47** (2007) S203.

[2] M.Y. Ye, S. Takamura and N. Ohno, J. Nucl. Mater. **241-243** (1997) 1243.

[3] S. Takamura, N. Ohno, D. Nishijima and S. Kajita, Plasma Fusion Res. **1** (2006) 051.

[4] S. Kajita, S. Takamura and N. Ohno, Nucl. Fusion **49** (2009) 032002.

[5] S.Takamura et al., "Compact Plasma Device for PWI Studies", accepted for publication in J.Plasma Fusion Res. SERIES,

[6] D. Nishijima, M.Y. Ye, N. Ohno and S. Takamura, Proc. 30th EPS Conf. on Contr. Fusion and Plasma Phys., St. Petersburg, ECA **Vol.27A** (2003) 2.163.

[7] D. Nishijima, M.Y. Ye, N. Ohno and S. Takamura,, J. Nucl.

Mater. **313-316** (2003) 97.

[8] D. Nishijima, M.Y. Ye, N. Ohno and S. Takamura,, J. Nucl. Mater. **329-333** (2004) 1029.

[9] M.Y. Ye, S. Fukuta, N. Ohno, S. Takamura, K. Tokunaga and N. Yoshida, J. Plasma Fusion Res. SERIES **3** (2000) 265.

[10] W. Sakaguchi, S. Kajita, N. Ohno and M. Takagi, J. Nucl. Mater. **290-391** (2009) 1149.

[11] S. Kajita, S. Takamura, N. Ohno, D. Nishijima, H. Iwakiri and N. Yoshida, Nucl. Fusion **47** (2007) 1358.